

Comparison of diffusion-weighted MRI acquisition techniques for normal pancreas at 3.0 Tesla

Xiu-Zhong Yao, Tiantao Kuang, Li Wu, Hao Feng, Hao Liu, Wei-Zhong Cheng, Sheng-Xiang Rao, He Wang, Meng-Su Zeng

PURPOSE

We aimed to optimize diffusion-weighted imaging (DWI) acquisitions for normal pancreas at 3.0 Tesla.

MATERIALS AND METHODS

Thirty healthy volunteers were examined using four DWI acquisition techniques with b values of 0 and 600 s/mm² at 3.0 Tesla, including breath-hold DWI, respiratory-triggered DWI, respiratory-triggered DWI with inversion recovery (IR), and free-breathing DWI with IR. Artifacts, signal-to-noise ratio (SNR) and apparent diffusion coefficient (ADC) of normal pancreas were statistically evaluated among different DWI acquisitions.

RESULTS

Statistical differences were noticed in artifacts, SNR, and ADC values of normal pancreas among different DWI acquisitions by ANOVA ($P < 0.001$). Normal pancreas imaging had the lowest artifact in respiratory-triggered DWI with IR, the highest SNR in respiratory-triggered DWI, and the highest ADC value in free-breathing DWI with IR. The head, body, and tail of normal pancreas had statistically different ADC values on each DWI acquisition by ANOVA ($P < 0.05$).

CONCLUSION

The highest image quality for normal pancreas was obtained using respiratory-triggered DWI with IR. Normal pancreas displayed inhomogeneous ADC values along the head, body, and tail structures.

Diffusion-weighted magnetic resonance imaging (DW-MRI) has increasingly expanded to abdominal organs thanks to newer technical developments. Diffusion-weighted imaging (DWI) can provide great details of functional and anatomic information that can be used in the differential diagnosis of abdominal pathological conditions. Investigators have recently reported that DWI can be utilized to detect pancreatic cancer (1, 2) and analysis of apparent diffusion coefficient (ADC) can help differentiate pancreatic masses (3–6). The single-shot spin-echo echo-planar imaging combined with parallel imaging technique is commonly employed for pancreatic DWI studies. Breath-hold DWI is the most common technique used for signal acquisition, especially on 1.5 Tesla (T) magnetic resonance (MR) system, because of its time efficiency. However, there are several disadvantages of breath-hold DWI, including poor signal-to-noise ratio (SNR), limited scan volume and significant artifacts (7, 8). Respiratory-triggered and free-breathing techniques are also used for signal acquisition in pancreatic DWI studies. Compared to breath-hold, the advantages of respiratory-triggered and free-breathing techniques are higher SNR due to multiple signal acquisitions, larger scanning range and less artifacts; their main disadvantage being the longer scanning time (9). Additionally, techniques of fat suppression, such as chemical shift selective (CHESS) and short tau inversion recovery, are essential for DWI in the pancreas for improving the contrast ratio and contrast-to-noise ratio of lesions with respect to normal pancreatic tissues (1, 6, 10).

Previously, most investigations were performed using 1.5 T MR scanners. Pancreas imaging using DWI with 3.0 T MR system needs to be further clarified and understood due to its increasing application, which may be a challenging task because of specific absorption rate and various artifacts from high sensitivity to magnetic field inhomogeneity and physiological movement (11). The aim of this study was to investigate different DWI techniques to visualize normal pancreas using a 3.0 T MR scanner and determine the best image acquisition technique in terms of artifacts, SNR, and ADC.

Materials and methods

The institutional review board approved this study, and written informed consent was obtained from all subjects.

Study participants

From May 2010 to May 2013, 30 healthy volunteers (19 men and 11 women; median age, 49.5 years; 1st quartile–3rd quartile age, 37.5–58.5 years) were enrolled. Healthy adults aged 30–70 years were included;

From the Department of Radiology (X-Z.Y., L.W., H.F., H.L., W-Z.C., S-X.R., M-S.Z. ✉ zengmengsu@gmail.com), Zhongshan Hospital of Fudan University, Shanghai, China; the Department of Medical Imaging (X-Z.Y., L.W., H.F., H.L., W-Z.C., S-X.R., M-S.Z.), Shanghai Institute of Medical Imaging, Shanghai Medical College of Fudan University, Shanghai, China; the Department of General Surgery (T.K.), Zhongshan Hospital of Fudan University, Shanghai, China; Global Applied Science Laboratory (H.W.), GE Healthcare, Shanghai, China.

Received 22 November 2013; revision requested 17 December 2013; final revision received 20 February 2014; accepted 24 February 2014.

Published online 19 June 2014.
DOI 10.5152/dir.2014.13454

Xiu-Zhong Yao and Tiantao Kuang contributed equally to this work.

volunteers with circulatory diseases and history of long-term medication therapy were excluded.

Imaging protocol

All healthy volunteers were examined in the supine position with a 3.0 T MR scanner (Signa HDx, GE Healthcare, Milwaukee, Wisconsin, USA) using an abdominal surface coil. The following four DWI acquisition techniques using motion-probing gradient (MPG) pulses on X, Y, Z direction based on spin-echo echo-planar imaging sequence with b values of 0 and 600 s/mm² were utilized: breath-hold DWI, respiratory-triggered DWI, respiratory-triggered DWI with inversion recovery (IR), and free-breathing DWI with IR. The parameters for those four DWI acquisition techniques are outlined in Table 1. The routine imaging protocol comprised an axial T2-weighted imaging using a fast spin-echo sequence (TR/TE, 4500/88 ms; flip angle, 90°; slice thickness/gap, 5/2 mm; bandwidth, 83.3 kHz; field of view, 400 mm²; matrix, 320×224 mm), an axial T1-weighted imaging using a fast spoiled gradient-echo sequence (TR/TE, 285/2.1 ms; flip angle, 60°; slice thickness/gap, 5/2 mm; bandwidth, 83.3 kHz; field of view, 400 mm²; matrix, 192×256 mm), and a coronal thick-section MR cholangiopancreatography using a single-shot fast spin-echo (TR/TE, 7000/1228 ms; flip angle, 90°; slice thickness/gap, 50/0 mm; bandwidth, 83.3 kHz; field of view, 300 mm²; matrix, 288×288 mm).

Image analysis

All pancreatic images from DWI were evaluated by two experienced radiologists (eight and seven years of experience in abdominal MRI, respectively) with reference to other sequences such as T1WI and T2WI. When the two radiologists disagreed, a senior radiologist (14 years of experience in abdominal MRI) was consulted. Images of 30 healthy volunteers were used for comparison of artifact scores, SNR, and ADC of normal pancreas among different DWI acquisition techniques. All investigators were blinded to the parameters used in DWI sequences.

Qualitative image analysis

Artifacts on all images were graded by two reviewers on a 4-point scale: 0, no

Table 1. Parameters of four DWI acquisition techniques on pancreas

	BH-DWI	TRIG-DWI	TRIGIR-DWI	FBIR-DWI
TR (ms)	2300	7500	7500	8000
TE (ms)	52	60	60	60
Asset factor	2	2	2	2
NEX	4	6	6	6
Bandwidth (kHz)	250	250	250	250
Field of view (mm)	400×280	400×280	400×280	400×280
Matrix size (mm)	130×96	130×96	130×96	130×96
Inversion time (ms)	NA	NA	220	220
Slice thickness/gap (mm)	5/2	5/2	5/2	5/2
Maximum slices	14	25	25	25
Scanning time (s)	18	163	163	141

DWI, diffusion-weighted imaging; BH, breath-hold; TRIG, respiratory-triggered; TRIGIR, respiratory-triggered inversion recovery; FBIR, free-breathing inversion recovery; TR, repetition time; TE, echo time; NEX, number of excitations.

artifacts; 1, mild artifacts (observable for DWI images and feasible for ADC measurements); 2, moderate artifacts (observable for DWI images and infeasible for ADC measurements); and 3, severe artifacts (unobservable for DWI images and infeasible for ADC measurements). Each slice (containing pancreatic tissues) of DWI images for each subject was graded and summarized, and mean artifact score was computed and recorded for each subject. The artifacts were categorized into the following three groups: (1), ghost/motion artifacts mainly from physiological movement around the pancreas, such as periodic and respiratory motion or gastrointestinal motility; (2), susceptibility or eddy-current induced artifacts, demonstrated as signal loss or distortion of structures at tissue-air interfaces; (3), radiofrequency inhomogeneity artifacts due to dielectric effect or eddy-current, such as the dark area on DWI images. The investigators also subjectively evaluated the image quality in terms of signal features and depiction of normal pancreas (blurry or sharp margins) on different DWI acquisitions.

Quantitative image analysis

Image processing was performed on a workstation (GE Medical Systems, ADW 4.3 version). A freehand region-of-interest (ROI, along the border of normal pancreas) was respectively drawn on the head, body, and tail of normal pancre-

as on different slices of different images obtained by DWI. The selected image contained the largest part of pancreas. Artifacts and main pancreatic duct were avoided. The SNR of the targeted pancreas was calculated for different DWI acquisitions according to the following equation: $SNR = SI / SD_{noise}$, where SI is the signal intensity and SD_{noise} is the standard deviation of background noise. The signal of background noise was calculated and averaged by respectively drawing three ROIs of approximately 1 cm² in an artifact-free part outside the abdominal wall on the phase direction. The SNR of normal pancreas for each subject was averaged from the SNR of pancreatic head, body, and tail. The ADC values of pancreas was automatically obtained from pixel-by-pixel calculation of pancreatic signal intensity using the following equation: $ADC = \ln[S_1/S_2] / (b_2 - b_1)$, where S_1 and S_2 are the signal intensities of pancreas measured on images with a lower b factor ($b_1 = 0$ s/mm²) and a higher b factor ($b_2 = 600$ s/mm²), respectively. The ADC values of the head, body, and tail of pancreas were obtained through the correspondingly drawn ROIs. The ADC value of pancreas for each subject was averaged through ADC values of pancreatic head, body, and tail.

Statistical analysis

Statistical analyses were performed using SPSS for Windows, version 16.0 (SPSS Inc, Chicago, Illinois, USA). Nor-

mal distribution and homogeneity of variance were tested for all parameters before conducting further tests. Square root transformation was used if normal distribution and homogeneity of variance conditions were not met. Artifact scores, SNR, and ADC values of normal pancreas were investigated and compared among different DWI acquisitions by repeated measures ANOVA and the paired Student t-test with Bonferroni correction. Statistical analysis of ADC values obtained through different DWI acquisitions was performed using ANOVA and the paired Student t-test with Bonferroni correction. A statistical difference was reached if the *P* value was less than 0.05.

Results

Normal pancreas displayed homogeneous hypointensity and sharp margins on respiratory-triggered DWI with IR (Fig. 1); homogeneous hypointensity, but blurry margins on free-breathing DWI with IR (Fig. 2); heterogeneous signal intensity (low to high signal intensity), but relatively clear margins on respiratory-triggered DWI (Fig. 3); and heterogeneous signal intensity (low to high signal intensity), but relatively clear margins on breath-hold DWI (Fig. 4). However, distortion and absence of normal pancreas was often observed on breath-hold DWI.

Artifact scores showed statistical difference among different DWI acquisitions with *b* values of 0 and 600 s/mm² by repeated measures ANOVA (*P* < 0.001). Lowest artifact scores for normal pancreas were obtained on respiratory-triggered DWI with IR, followed by free-breathing DWI with IR, respiratory-triggered DWI, and breath-hold DWI (Table 2). Fisher's least significant difference test showed no significant difference between pairwise comparisons of artifact scores obtained on respiratory-triggered DWI with IR, free-breathing DWI with IR, and respiratory-triggered DWI; however, all three acquisition techniques yielded significantly lower artifact scores than breath-hold DWI (*P* < 0.001, *P* = 0.008, and *P* = 0.013, respectively). The SNR of normal pancreas was significantly different among different DWI acquisition techniques by repeated measures ANOVA (*P* < 0.001):

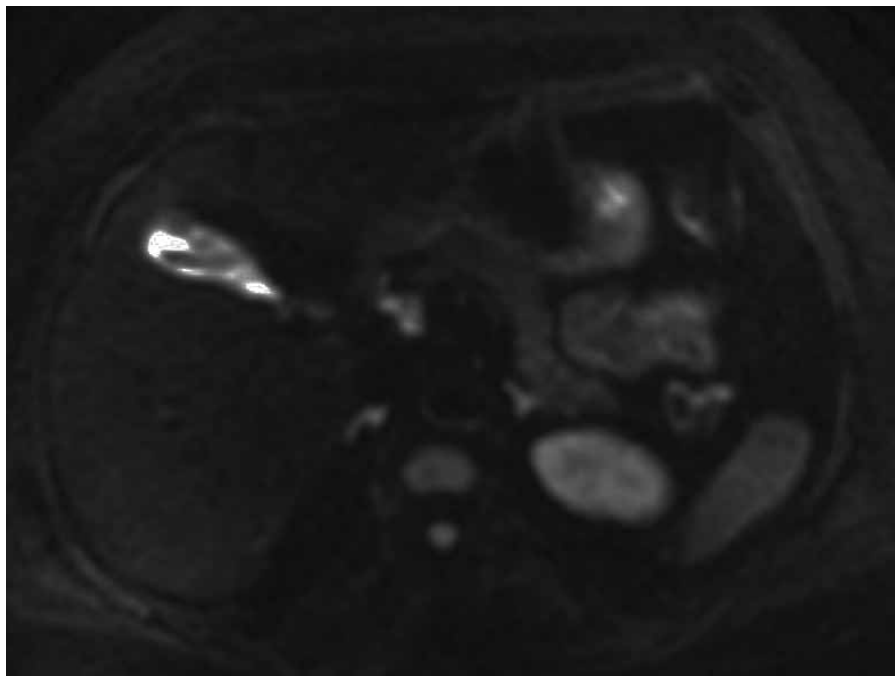


Figure 1. Respiratory-triggered DWI with inversion recovery technique showing normal pancreas with sharp margins and homogeneous hypointensity.

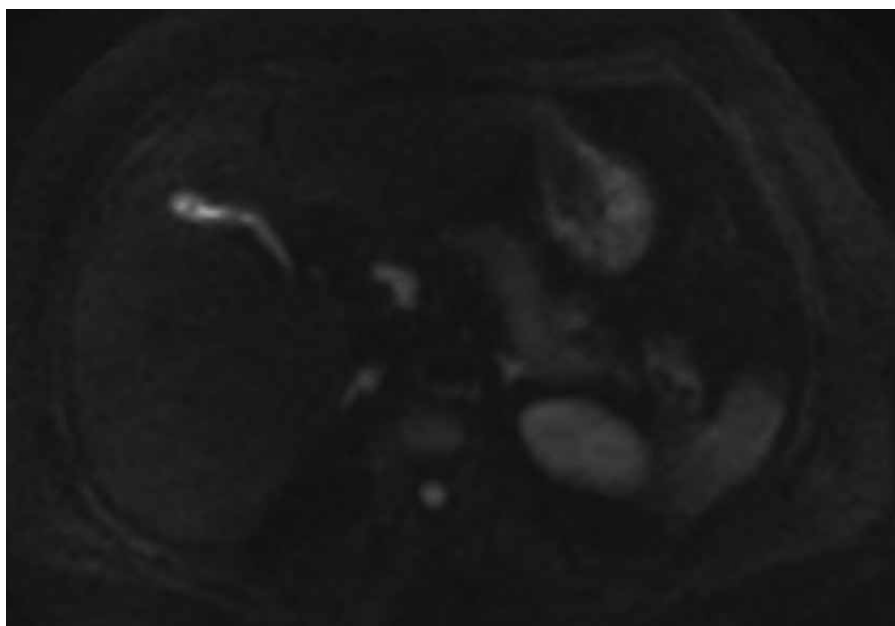


Figure 2. Free-breathing DWI with inversion recovery technique showing normal pancreas with homogeneous hypointensity, but blurry margins.

respiratory-triggered DWI yielded the highest SNR, followed by breath-hold DWI, respiratory-triggered DWI with IR and free-breathing DWI with IR (Table 2). The SNR values were significantly higher on respiratory-triggered DWI acquisition compared with respiratory-triggered DWI with IR and free-breathing DWI with IR (*P* < 0.001, for both). Similarly, SNR values were

significantly higher using breath-hold DWI compared with respiratory-triggered DWI with IR and free-breathing DWI with IR (*P* < 0.001). There was no significant difference between respiratory-triggered DWI and breath-hold DWI regarding the SNR of normal pancreas. Repeated measures ANOVA revealed significant differences in ADC values of normal pancreas among four

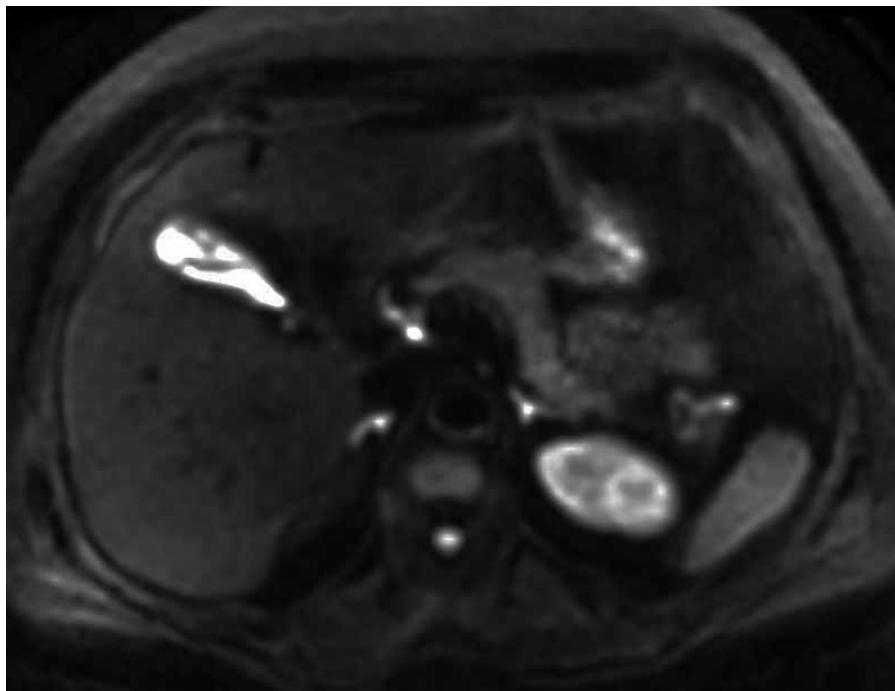


Figure 3. Respiratory-triggered DWI showing normal pancreas with heterogeneous signal intensity (iso- to hyperintensity), but relatively clear margins.

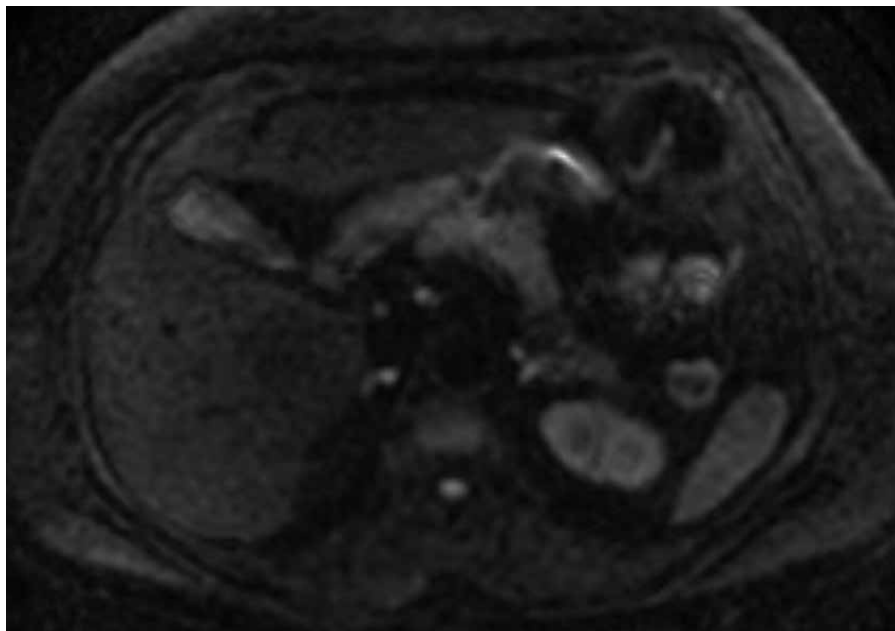


Figure 4. Breath-hold DWI showing normal pancreas with heterogeneous signal intensity (hypo- to hyperintensity), but relatively clear margins.

different DWI acquisition techniques ($P < 0.001$): free-breathing DWI with IR yielded the highest ADC value, followed by respiratory-triggered DWI with IR, respiratory-triggered DWI, and breath-hold DWI (Table 2). Respiratory-triggered DWI had significantly different ADC value of normal pancreas compared with free-breathing DWI

with IR ($P = 0.009$) and breath-hold DWI ($P = 0.007$). Respiratory-triggered DWI with IR had significantly different ADC value of normal pancreas compared with breath-hold DWI ($P < 0.001$), but not with free-breathing DWI with IR ($P = 0.896$). Free-breathing DWI with IR had significantly different ADC value of normal pancreas

compared with breath-hold DWI ($P < 0.001$).

Statistically significant differences in ADC values of the head, body and tail of normal pancreas were observed on each DWI acquisition by ANOVA ($P < 0.05$). The head of normal pancreas had the lowest ADC value compared with the body and tail of normal pancreas. The ADC values were statistically different between the head and tail of pancreas on each DWI sequence ($P < 0.017$), but not between the body and tail of pancreas. Statistically significant differences were observed between ADC values of the head and body of normal pancreas in images acquired on breath-hold DWI, respiratory-triggered DWI with IR, and free-breathing DWI with IR ($P < 0.05$), but not on respiratory-triggered DWI (Table 3).

Discussion

Respiratory-triggered DWI with IR was determined to be the optimal acquisition for normal pancreas in this study, as it yielded the highest image quality and helped better depict pancreas using a 3.0 T MR system. It is extremely important to make normal pancreas appear dark (hypointense) on DWI by decreasing the signal intensity of normal pancreas using the IR technique, because hypointense normal pancreas produces the highest contrast ratio of pancreatic cancer to noncancerous tissues, facilitating tumor detection. Some investigators favor breath-hold technique for pancreas (12, 13). However, its image quality can be degraded by several factors, such as cardiac and respiratory motion, susceptibility artifacts at tissue-air interfaces, blurring due to a long readout interval, and any motion during the data collection period (e.g., peristalsis). Other investigators favor respiratory-triggered and free-breathing DWI combined with fat-suppression techniques because its image quality might be superior to breath-hold DWI owing to the enlarged scan volume and decreased artifacts in spite of its longer imaging time (1, 6, 14, 15). The primary aim of IR pulse before MPG pulses was to lower the signal intensity of pancreas and suppress the signal intensity of surrounding fat at 3.0 T MR. The disad-

Table 2. Artifact scores, SNR, and ADC values of normal pancreas using different DWI acquisition techniques

	BH-DWI	TRIG-DWI	TRIGIR-DWI	FBIR-DWI
Artifact scores	1.05±0.38	0.67±0.42	0.39±0.28	0.65±0.41
SNR	60.67±19.18	70.75±25.49	26.15±10.38	22.59±10.10
ADC values (10 ⁻³ mm ² /s)	1.50±0.37	1.64±0.31	1.83±0.25	1.84±0.27

SNR, signal to noise ratio; ADC, apparent diffusion coefficient; DWI, diffusion-weighted imaging; BH, breath-hold; TRIG, respiratory-triggered; TRIGIR respiratory-triggered inversion recovery; FBIR, free-breathing inversion recovery.

Table 3. Heterogeneity of ADC values of normal pancreas on DWI acquisitions

	Pancreas regions	ADC values (10 ⁻³ mm ² /s)	<i>P</i>
BH-DWI	Head ^{a, b}	1.19±0.31	0.0003
	Body ^a	1.61±0.27	
	Tail ^b	1.69±0.34	
TRIG-DWI	Head ^b	1.49±0.19	0.031
	Body	1.69±0.32	
	Tail ^b	1.75±0.39	
TRIGIR-DWI	Head ^{a, b}	1.69±0.13	0.005
	Body ^a	1.95±0.31	
	Tail ^b	1.88±0.19	
FBIR-DWI	Head ^{a, b}	1.61±0.19	0.0004
	Body ^a	1.91±0.26	
	Tail ^b	1.96±0.27	

ADC, apparent diffusion coefficient; DWI, diffusion-weighted imaging; BH, breath-hold; TRIG, respiratory-triggered; TRIGIR, respiratory-triggered inversion recovery; FBIR, free-breathing inversion recovery. ^a*P* < 0.05 for head and body of pancreas; ^b*P* < 0.05 for head and tail of pancreas.

respiratory-triggered DWI with IR and free-breathing DWI with IR, which might be due to their similar effects on ADC measurements. Also, 220 ms of inversion time before MPG pulses at 3.0 T MR with the above IR techniques could cause an elevation of ADC values of normal pancreas. Both Braithwaite et al. (21) and Schoennagel et al. (22) reported heterogeneous ADC values among the pancreatic head, body, and tail regions observed using either a 1.5 T or 3.0 T MR scanner. However, Barral et al. (23) demonstrated a homogeneous ADC distribution among different pancreatic regions at 3.0 T, which is different from conclusions of our study. On all DWI acquisitions in this study, pancreatic head displayed the lowest ADC values compared with the pancreatic body and tail, which could be due to higher density of neuroendocrine cells distributed in the body and tail of normal pancreas.

This study had certain limitations. First, multiple b values were not used for each DWI acquisition technique; thus our results might be biased by the chosen b value if optimal b values are over 600 s/mm². Second, CHES was not utilized for fat suppression in this study. The main disadvantage of CHES is its sensitivity to B₀ and B₁ inhomogeneities. The failure to suppress subcutaneous fat using CHES induced multiple band-like and bright artifacts with high signal intensity on phase direction, which often covered the normal pancreas in this study. In contrast, the primary advantage of inversion-recovery technique for fat-suppression, including subcutaneous and pancreas-surrounding fat, lied in its ability to produce uniform suppression due to its strong insensitivity to B₀ and B₁ inhomogeneities. Additionally, inversion-recovery technique could be further used to partly and homogeneously suppress the signal intensity of normal pancreas, which aided to detect pancreatic lesions. Third, the inter- and intraobserver reliability and consistency was not tested for qualitative and quantitative analysis among different DWI acquisitions. The main purpose of this study was to investigate and compare different DWI acquisitions of normal pancreas, but not the usefulness of a single DWI acquisition. Additionally,

vantage of DWI with IR technique was loss of SNR in pancreatic tissues. The SNR in breath-hold DWI and respiratory-triggered DWI without IR technique was higher than respiratory-triggered or free-breathing DWI with IR technique; SNR of the latter two could be improved by multiple signal acquisitions. The T1 relaxation time of the pancreas and fat at 3.0 T MR was measured as approximately 725 and 382 ms, respectively (16). In order to minimize background noise and scanning time, 220 ms was used as the inversion time in this study. Furthermore, free-breathing DWI with IR and respiratory-triggered DWI with IR at a 3.0 T MR system could enlarge scan volume and reduce artifacts. Compared to breath-hold DWI, respiratory-triggered DWI, with or without IR, and free-breathing DWI with IR displayed the least artifacts on normal pancreas.

Artifacts of free-breathing DWI with IR were mostly from respiratory motion.

There are many factors that affect the signal intensity on DWI and affect measured ADC values, such as b values, magnetic strength, signal acquisitions, artifacts, cellular density, fiber content, the degree of blood supply or post-processing working stations (4, 17–20). For normal pancreas, ADC values were different among different DWI acquisitions (except for respiratory-triggered DWI with IR and free-breathing DWI with IR) and on different parts of normal pancreas (except for the body and tail of pancreas) in this study. Breath-hold DWI yielded the lowest ADC values of normal pancreas, probably because respiratory motion could lead to pseudo-movement of water molecules. There was no statistical difference between ADC values of normal pancreas obtained by

the baseline of probable errors in qualitative and quantitative analysis among different DWI acquisitions might be similar, because all image grading and ROI-related measurements were performed by the same two experienced investigators and further verified by the same senior abdominal radiologist when necessary. Furthermore, all readers were blinded to the details of parameters on different images.

In conclusion, respiratory-triggered DWI with IR provides superior image quality for normal pancreas compared with the other three DWI techniques at a 3.0 T MR scanner. Normal pancreas demonstrates heterogeneous ADC values, with the pancreatic head showing the lowest ADC value.

Financial disclosure

Supported by grants from the Shanghai Natural Science Foundation of China (12ZR1429600).

Conflict of interest disclosure

The authors declared no conflicts of interest.

References

- Hikawa T, Erturk SM, Motosugi U, et al. High-b value diffusion-weighted MRI for detecting pancreatic adenocarcinoma: preliminary results. *AJR Am J Roentgenol* 2007; 188:409–414. [\[CrossRef\]](#)
- Takakura K, Sumiyama K, Munakata K, et al. Clinical usefulness of diffusion-weighted MR imaging for detection of pancreatic cancer: comparison with enhanced multidetector-row CT. *Abdom Imaging* 2011; 36:457–462. [\[CrossRef\]](#)
- Inan N, Arslan A, Akansel G, Anik Y, Demirci A. Diffusion-weighted imaging in the differential diagnosis of cystic lesions of the pancreas. *AJR Am J Roentgenol* 2008; 191:1115–1121. [\[CrossRef\]](#)
- Wang Y, Miller FH, Chen ZE, et al. Diffusion-weighted MR imaging of solid and cystic lesions of the pancreas. *Radiographics* 2011; 31:47–64. [\[CrossRef\]](#)
- Irie H, Honda H, Kuroiwa T, et al. Measurement of the apparent diffusion coefficient in intraductal mucin-producing tumor of the pancreas by diffusion-weighted echo-planar MR imaging. *Abdom Imaging* 2002; 27:82–87. [\[CrossRef\]](#)
- Kartalis N, Lindholm TL, Aspelin P, Permert J, Albiin N. Diffusion-weighted magnetic resonance imaging of pancreas tumours. *Eur Radiol* 2009; 19:1981–1990. [\[CrossRef\]](#)
- Kartalis N, Loizou L, Edsborg N, Segersvard R, Albiin N. Optimising diffusion-weighted MR imaging for demonstrating pancreatic cancer: a comparison of respiratory-triggered, free-breathing and breath-hold techniques. *Eur Radiol* 2012; 22:2186–2192. [\[CrossRef\]](#)
- Kandpal H, Sharma R, Madhusudhan KS, Kapoor KS. Respiratory-triggered versus breath-hold diffusion-weighted MRI of liver lesions: comparison of image quality and apparent diffusion coefficient values. *AJR Am J Roentgenol* 2009; 19:915–922. [\[CrossRef\]](#)
- Perman WH, Balci NC, Akduman I, Kuntz E. Magnetic resonance measurement of diffusion in the abdomen. *Top Magn Reson Imaging* 2009; 20:99–104. [\[CrossRef\]](#)
- Lee SS, Byun JH, Park BJ, Kapoor KS. Quantitative analysis of diffusion-weighted magnetic resonance imaging of the pancreas: usefulness in characterizing solid pancreatic masses. *J Magn Reson Imaging* 2008; 28:928–936. [\[CrossRef\]](#)
- Saremi F, Jalili M, Sefidbakht S, et al. Diffusion-weighted imaging of the abdomen at 3 T: image quality comparison with 1.5-T magnet using 3 different imaging sequences. *J Comput Assist Tomogr* 2011; 35:317–325. [\[CrossRef\]](#)
- Fattahi R, Balci NC, Perman WH, et al. Pancreatic diffusion-weighted imaging (DWI): comparison between mass-forming focal pancreatitis (FP), pancreatic cancer (PC), and normal pancreas. *J Magn Reson Imaging* 2009; 29:350–356. [\[CrossRef\]](#)
- Ma C, Pan CS, Zhang HG, et al. Diffusion-weighted MRI of the normal adult pancreas: the effect of age on apparent diffusion coefficient values. *Clin Radiol* 2013; 68:e532–e537. [\[CrossRef\]](#)
- Matsuki M, Inada Y, Nakai G, et al. Diffusion-weighted MR imaging of pancreatic carcinoma. *Abdom Imaging* 2007; 32:481–483. [\[CrossRef\]](#)
- Takeuchi M, Matsuzaki K, Kubo H, Nishitani H. High-b-value diffusion-weighted magnetic resonance imaging of pancreatic cancer and mass-forming chronic pancreatitis: preliminary results. *Acta Radiol* 2008; 49:383–386. [\[CrossRef\]](#)
- de Bazelaire CM, Duhamel GD, Rofsky NM, Alsop DC. MR imaging relaxation times of abdominal and pelvic tissues measured in vivo at 3.0 T: preliminary results. *Radiology* 2004; 230:652–659. [\[CrossRef\]](#)
- Sasaki M, Yamada K, Watanabe Y, et al. Variability in absolute apparent diffusion coefficient values across different platforms may be substantial: a multivendor, multi-institutional comparison study. *Radiology* 2008; 249: 624–630.
- Kivrak AS, Paksoy Y, Erol C, Koplay M, Ozbek S, Kara F. Comparison of apparent diffusion coefficient values among different MRI platforms: a multicenter phantom study. *Diagn Interv Radiol* 2013; 19:433–437. [\[CrossRef\]](#)
- Koinuma M, Ohashi I, Hanafusa K, Shibuya H. Apparent diffusion coefficient measurements with diffusion-weighted magnetic resonance imaging for evaluation of hepatic fibrosis. *J Magn Reson Imaging* 2005; 22:80–85. [\[CrossRef\]](#)
- Dale BM, Braithwaite AC, Boll DT, Merkle EM. Field strength and diffusion encoding technique affect the apparent diffusion coefficient measurements in diffusion-weighted imaging of the abdomen. *Invest Radiol* 2010; 45:104–108. [\[CrossRef\]](#)
- Braithwaite AC, Dale BM, Boll DT, Merkle EM. Short- and midterm reproducibility of apparent diffusion coefficient measurements at 3.0-T diffusion-weighted imaging of the abdomen. *Radiology* 2009; 250:459–465. [\[CrossRef\]](#)
- Schoennagel BP, Habermann CR, Roesch M, et al. Diffusion-weighted imaging of the healthy pancreas: apparent diffusion coefficient values of the normal head, body, and tail calculated from different sets of b-values. *J Magn Reson Imaging* 2011; 34:861–865. [\[CrossRef\]](#)
- Barral M, Soyer P, Ben Hassen W, et al. Diffusion-weighted MR imaging of the normal pancreas: reproducibility and variations of apparent diffusion coefficient measurement at 1.5- and 3.0-Tesla. *Diagn Interv Imaging* 2013; 94:418–427. [\[CrossRef\]](#)